

Sector Decomposition

Gudrun Heinrich

*IPPP, Department of Physics, University of Durham,
South Road, Durham DH1 3LE, UK
gudrun.heinrich@durham.ac.uk*

Abstract

Sector decomposition is a constructive method to isolate divergences from parameter integrals occurring in perturbative quantum field theory. We explain the general algorithm in detail and review its application to multi-loop Feynman parameter integrals as well as infrared divergent phase-space integrals over real radiation matrix elements.

1 Introduction

Modern particle physics has reached a level of experimental accuracy in the percent range, and some present and future precision experiments require theoretical uncertainties to be at the permille level. This need for precise theory predictions has pushed forward the frontier for calculations of higher orders in perturbation theory considerably in recent years. The calculation of higher order corrections relies to a large extent on tree- or loop level Feynman diagrams, where the unobserved degrees of freedom, respectively the loop momenta, have to be integrated out. It is well known that these integrations become increasingly difficult at higher orders, as the dimensionality of the integration parameter space and/or the number of scales involved is growing. The intricacy is closely related to the fact that these integrals in general contain ultraviolet (UV) or infrared¹ (IR) divergences which need to be renormalised respectively factorised, because they hinder an immediate numerical evaluation of complicated expressions. The subtraction of these singularities becomes more and more cumbersome at higher orders, due to the fact that the divergences will be entangled in an increasingly complicated way.

For ultraviolet divergences, Bogoliubov, Parasiuk, Hepp and Zimmermann [1–3], established a subtraction scheme valid to all orders in perturbation theory. In fact, the original idea of sector decomposition goes back to the proof of the BPHZ theorem by Hepp [2], who used a decomposition of integration parameter space into certain sectors in order to disentangle overlapping ultraviolet singularities.

Concerning infrared divergences, the finiteness of sufficiently inclusive observables is guaranteed by the Kinoshita-Lee-Nauenberg theorem [4,5], but in most practical applications, more exclusive information about the final state is required, such that a subtraction scheme for IR divergences has to be established. A constructive scheme to do so to all orders in perturbation theory has not been formulated in full generality yet, at least in what concerns soft *and collinear* divergences. However, the sector decomposition algorithm as outlined below offers a constructive method to isolate these divergences from Feynman parameter integrals, which in principle is valid to all orders in perturbation theory.

For the subtraction of (soft) IR divergences, several approaches have been suggested. Early ones, which are based already on the subdivision of the integration parameter space into different sectors where the parameters go to zero in an ordered way, can be found e.g. in [6–10]. These sectors, associated with certain sets of one-particle irreducible subgraphs, are more advanced than the sectors needed in the UV case, and provide a resolution of the singularities without the need for an iterative procedure for diagrams with off-shell external momenta. Further, the so-called R^* -operation [11, 12] has been developed, which removes not only UV-divergences but also soft IR divergences by a procedure similar to the R -operation [1] in the UV case. For a review of these methods, see e.g. [13, 14].

Later, the decomposition into sectors has been employed to extract logarithmic mass singularities from massive multi-scale integrals in the high energy limit at two loops [15]. In [16], the concept of sector decomposition has been elaborated to a general algorithm in the context of dimensional regularisation, allowing to isolate ultraviolet as well as infrared singularities from parameter integrals in an automated way [17]. The algorithm also has been implemented in a public code available from [18].

¹We will use “infrared” to denote both soft and collinear divergences.

At next-to-leading order (NLO) in perturbation theory, the use of dimensional regularisation [19,20] and the universal infrared structure of gauge theories involving massless particles, like QED and QCD, allowed to establish a framework to isolate IR singularities analytically, leading to a multitude of phenomenological predictions. More recently, an increasing number of results at next-to-next-to-leading order (NNLO) has also become available, and quite a number of them made use of the sector decomposition technique to isolate infrared singularities or to check analytical results [21–42].

As most problems encountered in the calculation of perturbative higher order corrections can be reduced to the evaluation of multi-dimensional parameter integrals, the applicability of sector decomposition is quite universal.

1.1 Multi-loop diagrams

The first application of the algorithm presented in [16] was the numerical evaluation of massless two-loop box diagrams at certain Euclidean points². Pioneering the analytical calculation of two-loop box diagrams, the planar topology with light-like external legs has been calculated by V.A. Smirnov [43], the non-planar one by J.B. Tausk [44], where the numerical results obtained by sector decomposition served as an important check of the analytical calculation. For massless two-loop box diagrams with one off-shell leg, the numerical results of Ref. [16] were predictions which played a major role to validate the subsequent analytical calculations [45,46], finally allowing the calculation of the full two-loop QCD matrix element for $e^+e^- \rightarrow 3$ jets [47].

Subsequently, sector decomposition was used to check a considerable number of analytical results for two-loop [27, 34, 35, 48–52], three-loop [53–55] and four-loop [36, 51] diagrams³.

Sector decomposition also has been combined with other methods for an efficient numerical calculation of one-loop multi-leg amplitudes, first on a diagrammatic level in Refs. [56, 57], later for whole amplitudes in Refs. [58, 59]. The latter approach contains a combination of sector decomposition and contour deformation [60–63], which allows to integrate the Feynman parameter representation of an amplitude numerically in the physical region. It also contains the application of sector decomposition to phase space integrals, which will be discussed below. Similar ideas, i.e. the combination of sector decomposition and contour deformation, are employed in Refs. [42, 64] for the numerical evaluation of multi-loop Feynman diagrams with infrared and threshold singularities.

Ref. [25] describes the implementation of an algorithm based on sector decomposition to extract the $1/\epsilon$ poles as well as the large logarithms of type $\ln(s/M^2)$ in the high-energy limit, allowing to obtain the next-to-leading logarithmic electroweak corrections of multi-loop diagrams.

Despite its success in practical applications, until very recently there was no formal proof that a strategy for the iterated sector decomposition can always be found such that the iteration is guaranteed to stop. This gap has been filled in Ref. [18], by mapping the problem to Hironaka’s Polyhedra game [65]. The findings of Ref. [18] subsequently have been used to prove that the coefficients of the Laurent series representing Feynman integrals in the Euclidean region with rational values for all invariants are a special class of numbers known by mathematicians as periods [66].

²By “Euclidean” we mean that all kinematic invariants formed from external momenta are negative.

³In Refs. [27, 34–36] the checks have been performed with an implementation of sector decomposition by M. Czakon, independent from the one in [16].

Also on a more formal level, it is outlined in [67] that sector decomposition can be used to automate the renormalisation of quantum field theories, by mapping to the so-called Henge decomposition [68], which served to provide a simple proof of the BPHZ theorem [69]. This mapping also allowed to establish a direct correspondence between overlapping divergences in Feynman parameter space and in momentum space [67]. In this context, one should also mention the formulation of renormalisation using Hopf algebras [70], which provide a framework to describe the disentanglement of divergent subgraphs of Feynman diagrams.

1.2 Phase space integrals

After the results for various two-loop box diagrams had become available, the bottleneck to make progress in the calculation of differential NNLO cross sections for $1 \rightarrow 3$ or $2 \rightarrow 2$ processes was the complicated infrared singularity structure of phase space integrals over matrix elements for the real radiation of (doubly) unresolved massless particles. As these phase space integrals can be written as dimensionally regularised parameter integrals, sector decomposition can serve to factorise entangled singularity structures in the case of real radiation as well. This idea has first been presented in [71] and subsequently has been applied to calculate all master four-particle phase space integrals where up to two particles in the final state can become soft and/or collinear [21]. Shortly after, this approach has been extended to be applicable to exclusive final states as well by expressing the functions produced by sector decomposition in terms of distributions [22]. A rapid development [23, 24] led to the calculation of $e^+e^- \rightarrow 2\text{jets}$ at $\mathcal{O}(\alpha_s^2)$ [24]. Further elaboration on this approach resulted in the first fully differential program to calculate an NNLO cross section [26, 28] and has led to differential NNLO results for a number of processes meanwhile [29, 31, 38, 41].

2 Basic concepts

To introduce the subject, let us look at the simple example of a two-dimensional parameter integral of the following form:

$$I = \int_0^1 dx \int_0^1 dy x^{-1-a\epsilon} y^{-b\epsilon} \left(x + (1-x)y \right)^{-1}. \quad (1)$$

The integral contains a singular region where x and y vanish *simultaneously*, i.e. the singularities in x and y are *overlapping*. Our aim is to factorise the singularities for $x \rightarrow 0$ and $y \rightarrow 0$. Therefore we divide the integration range into two sectors where x and y are ordered (see Fig. 1)

$$I = \int_0^1 dx \int_0^1 dy x^{-1-a\epsilon} y^{-b\epsilon} \left(x + (1-x)y \right)^{-1} \underbrace{[\Theta(x-y)]}_{(1)} + \underbrace{[\Theta(y-x)]}_{(2)}.$$

Now we substitute $y = xt$ in sector (1) and $x = yt$ in sector (2) to remap the integration range to the unit square and obtain

$$I = \int_0^1 dx x^{-1-(a+b)\epsilon} \int_0^1 dt t^{-b\epsilon} \left(1 + (1-x)t \right)^{-1}$$

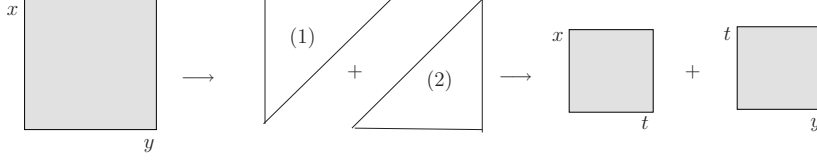


Figure 1: Sector decomposition schematically.

$$+ \int_0^1 dy y^{-1-(a+b)\epsilon} \int_0^1 dt t^{-1-a\epsilon} \left(1 + (1-y)t\right)^{-1}. \quad (2)$$

We observe that the singularities are now factorised such that they can be read off from the powers of simple monomials in the integration variables, while the polynomial denominator goes to a constant if the integration variables approach zero. The same concept will be applied to N -dimensional parameter integrals over polynomials raised to some power, where the procedure in general has to be iterated to achieve complete factorisation.

3 The algorithm for multi-loop integrals

3.1 Feynman parameter integrals

A general Feynman graph $G_{l_1 \dots l_R}^{\mu_1 \dots \mu_R}$ in D dimensions at L loops with N propagators and R loop momenta in the numerator, where the propagators can have arbitrary, not necessarily integer powers ν_j , has the following representation in momentum space:

$$G_{l_1 \dots l_R}^{\mu_1 \dots \mu_R} = \int \prod_{l=1}^L d^D \kappa_l \frac{k_{l_1}^{\mu_1} \dots k_{l_R}^{\mu_R}}{\prod_{j=1}^N P_j^{\nu_j}(\{k\}, \{p\}, m_j^2)}$$

$$d^D \kappa_l = \frac{\mu^{4-D}}{i\pi^{\frac{D}{2}}} d^D k_l, \quad P_j(\{k\}, \{p\}, m_j^2) = (q_j^2 - m_j^2 + i\delta), \quad (3)$$

where the q_j are linear combinations of external momenta p_i and loop momenta k_l . Introducing Feynman parameters according to

$$\frac{1}{\prod_{j=1}^N P_j^{\nu_j}} = \frac{\Gamma(N_\nu)}{\prod_{j=1}^N \Gamma(\nu_j)} \int_0^\infty \prod_{j=1}^N dx_j x_j^{\nu_j-1} \delta\left(1 - \sum_{i=1}^N x_i\right) \frac{1}{\left[\sum_{j=1}^N x_j P_j\right]^{N_\nu}}, \quad (4)$$

where $N_\nu = \sum_{j=1}^N \nu_j$, leads to

$$G_{l_1 \dots l_R}^{\mu_1 \dots \mu_R} = \frac{\Gamma(N_\nu)}{\prod_{j=1}^N \Gamma(\nu_j)} \int_0^\infty \prod_{j=1}^N dx_j x_j^{\nu_j-1} \delta\left(1 - \sum_{i=1}^N x_i\right) \int d^D \kappa_1 \dots d^D \kappa_L$$

$$k_{l_1}^{\mu_1} \dots k_{l_R}^{\mu_R} \left[\sum_{i,j=1}^L k_i^T M_{ij} k_j - 2 \sum_{j=1}^L k_j^T \cdot Q_j + J + i\delta \right]^{-N_\nu}, \quad (5)$$

where M is a $L \times L$ matrix containing Feynman parameters, Q is an L -dimensional vector composed of external momenta and Feynman parameters, and J contains kinematic invariants and Feynman parameters. The factors of $k_{l_i}^{\mu_i}$ in the numerator can be generated from $G(R=0)$ by partial differentiation with respect to $Q_l^{\mu_i}$, where $l \in \{1, \dots, L\}$ denotes the l^{th} component of the vector Q , corresponding to the l^{th} loop momentum. Therefore it is convenient to define the double indices $\Gamma_i = (l, \mu_i(l))$, $l \in \{1, \dots, L\}$, $i \in \{1, \dots, R\}$ denoting the i^{th} Lorentz index, belonging to the l^{th} loop momentum.

To perform the integration over the loop momenta k_l , we perform the following shift in order to obtain a quadratic form for the term in square brackets in eq. (5):

$$k'_l = k_l - v_l, \quad v_l = \sum_{i=1}^L M_{li}^{-1} Q_i. \quad (6)$$

After momentum integration one obtains

$$\begin{aligned} G_{l_1 \dots l_R}^{\mu_1 \dots \mu_R} &= (-1)^{N_\nu} \frac{1}{\prod_{j=1}^N \Gamma(\nu_j)} \int_0^\infty \prod_{j=1}^N dx_j x_j^{\nu_j-1} \delta(1 - \sum_{l=1}^N x_l) \\ &\quad \sum_{m=0}^{[R/2]} \left(-\frac{1}{2}\right)^m \Gamma(N_\nu - m - LD/2) \left[(\tilde{M}^{-1} \otimes g)^{(m)} \tilde{l}^{(R-2m)} \right]^{\Gamma_1, \dots, \Gamma_R} \\ &\quad \times \frac{\mathcal{U}^{N_\nu - (L+1)D/2 - R}}{\mathcal{F}^{N_\nu - LD/2 - m}} \end{aligned} \quad (7)$$

where

$$\begin{aligned} \mathcal{F}(\vec{x}) &= \det(M) \left[\sum_{j,l=1}^L Q_j M_{jl}^{-1} Q_l - J - i\delta \right] \\ \mathcal{U}(\vec{x}) &= \det(M) \\ \tilde{M}^{-1} &= \mathcal{U} M^{-1}, \quad \tilde{l} = \mathcal{U} v \end{aligned} \quad (8)$$

and $[R/2]$ denotes the nearest integer less or equal to $R/2$. The expression $[(\tilde{M}^{-1} \otimes g)^{(m)} \tilde{l}^{(R-2m)}]^{\Gamma_1, \dots, \Gamma_R}$ stands for the sum over all different combinations of R double-indices distributed to m metric tensors and $(R-2m)$ vectors \tilde{l} . The above expression is well known [14, 72–76], but an example to illustrate the distribution of indices may be helpful, so let us consider a two-loop integral where the k_1 -integral is a rank two tensor integral and the k_2 -integral is of rank one:

$$\begin{aligned} G_{112}^{\mu_1 \mu_2 \mu_3} &= \int d^D \kappa_1 d^D \kappa_2 \frac{k_1^{\mu_1} k_1^{\mu_2} k_2^{\mu_3}}{\prod_{j=1}^N P_j^{\nu_j}(\{k\}, \{p\}, m_j^2)} \\ &= \frac{(-1)^{N_\nu}}{\prod_{j=1}^N \Gamma(\nu_j)} \int_0^\infty \prod_{j=1}^N dx_j x_j^{\nu_j-1} \delta(1 - \sum_{l=1}^N x_l) \\ &\quad \left\{ \Gamma(N_\nu - D) \frac{\mathcal{U}^{N_\nu - 3D/2 - 3}}{\mathcal{F}^{N_\nu - D}} \tilde{l}_1^{\mu_1} \tilde{l}_1^{\mu_2} \tilde{l}_2^{\mu_3} \right. \\ &\quad \left. - \frac{1}{2} \Gamma(N_\nu - 1 - D) \frac{\mathcal{U}^{N_\nu - 3D/2 - 3}}{\mathcal{F}^{N_\nu - D - 1}} \times \right. \end{aligned} \quad (9)$$

$$\left[(\tilde{M}^{-1} \otimes g)_{11}^{\mu_1 \mu_2} \tilde{l}_2^{\mu_3} + (\tilde{M}^{-1} \otimes g)_{12}^{\mu_1 \mu_3} \tilde{l}_1^{\mu_2} + (\tilde{M}^{-1} \otimes g)_{12}^{\mu_2 \mu_3} \tilde{l}_1^{\mu_1} \right] \Big\} ,$$

$$(\tilde{M}^{-1} \otimes g)^{\mu\nu} = \begin{pmatrix} \tilde{M}_{11}^{-1} g^{\mu\nu} & \tilde{M}_{12}^{-1} g^{\mu\nu} \\ \tilde{M}_{21}^{-1} g^{\mu\nu} & \tilde{M}_{22}^{-1} g^{\mu\nu} \end{pmatrix} .$$

The functions \mathcal{U} and \mathcal{F} also can be constructed from the topology of the corresponding Feynman graph as follows [74, 77, 78]. Cutting L lines of a given connected L -loop graph such that it becomes a connected tree graph T defines a *chord* $\mathcal{C}(T)$ as being the set of lines not belonging to this tree. The Feynman parameters associated with each chord define a monomial of degree L . The set of all such trees (or *1-trees*) is denoted by \mathcal{T}_1 . The 1-trees $T \in \mathcal{T}_1$ define \mathcal{U} as being the sum over all monomials corresponding to a chord $\mathcal{C}(T \in \mathcal{T}_1)$. Cutting one more line of a 1-tree leads to two disconnected trees, or a *2-tree* \hat{T} . \mathcal{T}_2 is the set of all such 2-trees. The corresponding chords define monomials of degree $L + 1$. Each 2-tree of a graph corresponds to a cut defined by cutting the lines which connected the two now disconnected trees in the original graph. The momentum flow through the lines of such a cut defines a Lorentz invariant $s_{\hat{T}} = (\sum_{j \in \text{Cut}(\hat{T})} p_j)^2$. The function \mathcal{F}_0 is the sum over all such monomials times minus the corresponding invariant. For a diagram with massless propagators, $\mathcal{F} = \mathcal{F}_0$. If massive internal lines are present, \mathcal{F} gets an additional term as follows:

$$\begin{aligned} \mathcal{U}(\vec{x}) &= \sum_{T \in \mathcal{T}_1} \left[\prod_{j \in \mathcal{C}(T)} x_j \right] , \\ \mathcal{F}_0(\vec{x}) &= \sum_{\hat{T} \in \mathcal{T}_2} \left[\prod_{j \in \mathcal{C}(\hat{T})} x_j \right] (-s_{\hat{T}}) , \\ \mathcal{F}(\vec{x}) &= \mathcal{F}_0(\vec{x}) + \mathcal{U}(\vec{x}) \sum_{j=1}^N x_j m_j^2 . \end{aligned} \tag{10}$$

\mathcal{U} is a positive semi-definite function. Its vanishing is related to the UV subdivergences of the graph. Overall UV divergences, if present, will always be contained in the prefactor $\Gamma(N_\nu - LD/2)$. In the region where all invariants $s_{\hat{T}}$ are negative, which we will call the Euclidean region in the following, \mathcal{F} is also a positive semi-definite function of the Feynman parameters x_j . Its vanishing does not necessarily lead to an IR singularity. Only if some of the invariants are zero, for example if some of the external momenta are light-like, the vanishing of \mathcal{F} may induce an IR divergence. Thus it depends on the *kinematics* and not only on the topology (like in the UV case) whether a zero of \mathcal{F} leads to a divergence or not. This fact makes it much harder to formulate general theorems for the subtraction of IR singularities of multi-loop Feynman graphs. The necessary (but not sufficient) conditions for an IR divergence are given by the Landau equations [79–81], which, in parameter space, simply mean that the necessary condition $\mathcal{F} = 0$ for an IR divergence can only be fulfilled if some of the parameters x_i go to zero, provided that all kinematic invariants $s_{\hat{T}}$ are negative.

As can be seen from Eq. (7), the difference between scalar and tensor integrals is, once the Lorentz structure is extracted, given by the fact that there are polynomials of Feynman parameters in the numerator. These polynomials can simply be included into the sector decomposition procedure, thus treating tensor integrals directly without reduction to scalar integrals.

However, there is yet another possibility: Any tensor integral can be expressed in terms of scalar integrals in shifted dimensions, with some of the propagator powers different from unity, as has been shown in [75,78]. As our propagators can have arbitrary powers ν_j , and the dimension D is a free parameter, this is a viable alternative.

3.2 Iterated sector decomposition

For less trivial examples than the one given in section 2, the singularities will not be factorised already after a single step of sector decomposition. An algorithm how to iterate this procedure is described below.

Our starting point is a function of the form of Eq. (7). As the basic algorithm is the same for tensor integrals, we will consider $R = 0$ here for ease of notation, i.e.

$$G = (-1)^{N\nu} \frac{\Gamma(N\nu - LD/2)}{\prod_{j=1}^N \Gamma(\nu_j)} \int_0^\infty \prod_{j=1}^N dx_j x_j^{\nu_j-1} \delta(1 - \sum_{l=1}^N x_l) \frac{\mathcal{U}^{N\nu-(L+1)D/2}}{\mathcal{F}^{N\nu-LD/2}}. \quad (11)$$

Part I Generation of primary sectors

We split the integration domain into N parts and eliminate the δ -distribution in such a way that the remaining integrations are from 0 to 1. To this end we decompose the integration range into N sectors, where in each sector l , x_l is largest (note that the remaining $x_{j \neq l}$ are not further ordered):

$$\int_0^\infty d^N x = \sum_{l=1}^N \int_0^\infty d^N x \prod_{\substack{j=1 \\ j \neq l}}^N \theta(x_l \geq x_j). \quad (12)$$

The θ -function is defined as

$$\theta(x \geq y) = \begin{cases} 1 & \text{if } x \geq y \text{ is true} \\ 0 & \text{otherwise.} \end{cases}$$

The integral is now split into N domains corresponding to N integrals G_l from which we extract a common factor: $G = (-1)^{N\nu} \Gamma(N\nu - LD/2) \sum_{l=1}^N G_l$. In the integrals G_l we substitute

$$x_j = \begin{cases} x_l t_j & \text{for } j < l \\ x_l & \text{for } j = l \\ x_l t_{j-1} & \text{for } j > l \end{cases} \quad (13)$$

and then integrate out x_l using the δ -distribution. As \mathcal{U}, \mathcal{F} are homogeneous of degree $L, L+1$, respectively, and x_l factorises completely, we have $\mathcal{U}(\vec{x}) \rightarrow \mathcal{U}_l(\vec{t}) x_l^L$ and $\mathcal{F}(\vec{x}) \rightarrow \mathcal{F}_l(\vec{t}) x_l^{L+1}$ and thus, using $\int dx_l/x_l \delta(1 - x_l(1 + \sum_{k=1}^{N-1} t_k)) = 1$, we obtain

$$G_l = \int_0^1 \prod_{j=1}^{N-1} dt_j t_j^{\nu_j-1} \frac{\mathcal{U}_l^{N\nu-(L+1)D/2}(\vec{t})}{\mathcal{F}_l^{N\nu-LD/2}(\vec{t})}, \quad l = 1, \dots, N. \quad (14)$$

Note that the singular behaviour leading to $1/\epsilon$ -poles still comes from regions where a set of parameters $\{t_i\}$ goes to zero. This feature would be lost if the δ -distribution was integrated out in a different way, since this would produce poles at upper limits of the parameter integral as well. The N generated sectors will be called *primary* sectors in the following.

Part II Iteration

Starting from Eq. (14) we repeat the following steps until a complete separation of overlapping regions is achieved.

II.1: Determine a minimal set of parameters, say $\mathcal{S} = \{t_{\alpha_1}, \dots, t_{\alpha_r}\}$, such that \mathcal{U}_l , respectively \mathcal{F}_l , vanish if the parameters of \mathcal{S} are set to zero. \mathcal{S} is in general not unique, and there is no general prescription which defines what set to choose in order to achieve a *minimal* number of iterations. Strategies to choose \mathcal{S} such that the algorithm is guaranteed to stop are given in [18]. Using these strategies however in general leads to a larger number of iterations than heuristic strategies to avoid infinite loops, described in more detail below.

II.2: Decompose the corresponding r -cube into r *subsectors* by decomposing unity according to

$$\prod_{j=1}^r \theta(1 \geq t_{\alpha_j} \geq 0) = \sum_{k=1}^r \prod_{\substack{j=1 \\ j \neq k}}^r \theta(t_{\alpha_k} \geq t_{\alpha_j} \geq 0). \quad (15)$$

II.3: Remap the variables to the unit hypercube in each new subsector by the substitution

$$t_{\alpha_j} \rightarrow \begin{cases} t_{\alpha_k} t_{\alpha_j} & \text{for } j \neq k \\ t_{\alpha_k} & \text{for } j = k. \end{cases} \quad (16)$$

This gives a Jacobian factor of $t_{\alpha_k}^{r-1}$. By construction t_{α_k} factorises from at least one of the functions \mathcal{U}_l , \mathcal{F}_l . The resulting subsector integrals have the general form

$$G_{lk} = \int_0^1 \left(\prod_{j=1}^{N-1} dt_j t_j^{a_j - b_j \epsilon} \right) \frac{\mathcal{U}_{lk}^{N_\nu - (L+1)D/2}}{\mathcal{F}_{lk}^{N_\nu - LD/2}}, \quad k = 1, \dots, r. \quad (17)$$

For each subsector the above steps have to be repeated as long as a set \mathcal{S} can be found such that one of the functions $\mathcal{U}_{l\dots}$ or $\mathcal{F}_{l\dots}$ vanishes if the elements of \mathcal{S} are set to zero. This way new subsectors are created in each subsector of the previous iteration, resulting in a tree-like structure after a certain number of iterations. The iteration stops if the functions $\mathcal{U}_{lk_1 k_2 \dots}$ or $\mathcal{F}_{lk_1 k_2 \dots}$ contain a constant term, i.e. if they are of the form

$$\begin{aligned} \mathcal{U}_{lk_1 k_2 \dots} &= 1 + u(\vec{t}) \\ \mathcal{F}_{lk_1 k_2 \dots} &= -s_0 + \sum_{\beta} (-s_{\beta}) f_{\beta}(\vec{t}), \end{aligned} \quad (18)$$

where $u(\vec{t})$ and $f_{\beta}(\vec{t})$ are polynomials in the variables t_j (without a constant term), and s_{β} are kinematic invariants defined by the cuts of the diagram as explained above, or

(minus) internal masses. Thus, after a certain number of iterations, each integral G_l is split into a certain number, say α , of subsector integrals. We can replace the multi-index $k_1 k_2 \dots$ stemming from the subsector decomposition by a single index which just counts the number of generated subsectors. The subsector integrals are exactly of the same form as in Eq. (17), with the difference that the index k now runs from 1 to α , the total number of produced subsectors in each primary sector.

Evidently the singular behaviour of the integrand now can be read off directly from the exponents a_j, b_j for a given subsector integral. As the singular behaviour is manifestly non-overlapping now, it is straightforward to define subtractions.

Part III Extraction of the poles

The subtraction of the poles can be done implicitly by expanding the singular factors into distributions, or explicitly by direct integration over the singular factors. In any case, the following procedure has to be worked through for each variable $t_{j=1, \dots, N-1}$ and each subsector integrand:

- Let us consider Eq. (17) for a particular t_j , i.e. let us focus on

$$I_j = \int_0^1 dt_j t_j^{(a_j - b_j \epsilon)} \mathcal{I}(t_j, \{t_{i \neq j}\}, \epsilon), \quad (19)$$

where $\mathcal{I} = \mathcal{U}_{lk}^{N_\nu - (L+1)D/2} / \mathcal{F}_{lk}^{N_\nu - LD/2}$ in a particular subsector. If $a_j > -1$, the integration does not lead to an ϵ -pole. In this case no subtraction is needed and one can go to the next variable t_{j+1} . If $a_j \leq -1$, one expands $\mathcal{I}(t_j, \{t_{i \neq j}\}, \epsilon)$ into a Taylor series around $t_j = 0$:

$$\begin{aligned} \mathcal{I}(t_j, \{t_{i \neq j}\}, \epsilon) &= \sum_{p=0}^{|a_j|-1} \mathcal{I}_j^{(p)}(0, \{t_{i \neq j}\}, \epsilon) \frac{t_j^p}{p!} + R(\vec{t}, \epsilon), \text{ where} \\ \mathcal{I}_j^{(p)}(0, \{t_{i \neq j}\}, \epsilon) &= \left. \partial^p \mathcal{I}(t_j, \{t_{i \neq j}\}, \epsilon) / \partial t_j^p \right|_{t_j=0}. \end{aligned} \quad (20)$$

- Now the pole part can be extracted easily, and one obtains

$$I_j = \sum_{p=0}^{|a_j|-1} \frac{1}{a_j + p + 1 - b_j \epsilon} \frac{\mathcal{I}_j^{(p)}(0, \{t_{i \neq j}\}, \epsilon)}{p!} + \int_0^1 dt_j t_j^{a_j - b_j \epsilon} R(\vec{t}, \epsilon). \quad (21)$$

By construction, the integral containing the remainder term $R(\vec{t}, \epsilon)$ does not produce poles in ϵ upon t_j -integration anymore. For $a_j = -1$, which is the generic case for renormalisable theories (logarithmic divergence), this simply amounts to

$$I_j = -\frac{1}{b_j \epsilon} \mathcal{I}_j(0, \{t_{i \neq j}\}, \epsilon) + \int_0^1 dt_j t_j^{-1 - b_j \epsilon} \left(\mathcal{I}(t_j, \{t_{i \neq j}\}, \epsilon) - \mathcal{I}_j(0, \{t_{i \neq j}\}, \epsilon) \right),$$

which is equivalent to applying the “plus prescription” [82] (see eq. (45)), except that the integrations over the singular factors have been carried out explicitly.

Since, as long as $j < N - 1$, the expression (21) still contains an overall factor $t_{j+1}^{a_{j+1}-\epsilon b_{j+1}}$, it is of the same form as (19) for $j \rightarrow j + 1$ and the same steps as above can be applied.

After $N - 1$ steps all poles are extracted, such that the resulting expression can be expanded in ϵ . This defines a Laurent series in ϵ with coefficients $C_{lk,m}$ for each of the $\alpha(l)$ subsector integrals G_{lk} . Since each loop can contribute at most one soft and collinear $1/\epsilon^2$ term, the highest possible infrared pole of an L -loop graph is $1/\epsilon^{2L}$. Expanding to order ϵ^r , one has

$$G_{lk} = \sum_{m=-r}^{2L} \frac{C_{lk,m}}{\epsilon^m} + \mathcal{O}(\epsilon^{r+1}), \quad G = (-1)^{N_\nu} \Gamma(N_\nu - LD/2) \sum_{l=1}^N \sum_{k=1}^{\alpha(l)} G_{lk}. \quad (22)$$

Following the steps outlined above one has generated a regular integral representation of the coefficients $C_{lk,m}$, consisting of $(N - 1 - m)$ -dimensional finite integrals over parameters t_j . We recall that \mathcal{F} was non-negative in the Euclidean region where all invariants are negative (see eqs. (10,18)), such that the numerical integrations over the finite parameter integrals are straightforward in this region. In principle, it is also possible to do at least part of these parameter integrals analytically, but in most applications such an analytical approach reaches its limits very quickly.

Avoiding infinite recursion

As mentioned already, the choice of the set $\mathcal{S} = \{t_{\alpha_1}, \dots, t_{\alpha_r}\}$ which makes \mathcal{U} respectively \mathcal{F} vanish for $t_\alpha \rightarrow 0$ is in general not unique. The structure of the function \mathcal{U} (see eq. (10)) is such that its decomposition will always terminate after L iterations for an L -loop integral. For the function \mathcal{F} , the structure depends on the masses and kinematic invariants involved. Although one could follow one of the mathematical strategies given in [18] to ensure the iteration terminates, this is not the most efficient method for practical purposes, as these strategies typically generate a large number of subsectors. Another possibility, adopted in [25], is to choose the set \mathcal{S} randomly, such that eventually a set will be selected which does not lead to infinite recursion. However, it is more efficient to use some heuristic rules which, in all applications to multi-loop diagrams considered so far by the author, lead to a terminating decomposition procedure.

Let us first illustrate the problem by a simple example: Consider the function

$$f(x_1, x_2, x_3) = x_1^2 + x_2^2 x_3, \quad (23)$$

and suppose we choose $\mathcal{S} = \{1, 3\}$. The replacement $x_1 = x_3 t_1$ in the subsector associated with $\theta(x_3 - x_1)$ leads to $\tilde{f} = x_3 (x_3 t_1^2 + x_2^2)$. Choosing now $\mathcal{S} = \{2, 3\}$ and substituting $x_2 = x_3 t_2$ in the corresponding subsector brings us back to the original functional form, so we generate an infinite recursion for the above choices of \mathcal{S} . In this simple example we can see immediately that the choice $\mathcal{S} = \{1, 2\}$ does not lead to this problem.

For multi-loop integrals, we can use the following facts as a guideline to choose convenient sets \mathcal{S} : We first note that an infinite recursion does not occur for functions which are linear in each variable. The function \mathcal{F} , before the iterated decompositions, is a polynomial of maximal degree two in each individual Feynman parameter, where quadratic

parameters only occur if massive propagators are present, due to the term $\mathcal{U}(\vec{x}) \sum_{j=1}^N x_j m_j^2$ contained in \mathcal{F} (see eq.(10)). Therefore, a simple extra rule for diagrams with internal masses can be added to the procedure: Before entering the iteration, determine the set \mathcal{S}_M of labels belonging to massive propagators and use this set for a first sector decomposition (even if it does not lead to $\mathcal{F} = 0$ upon setting the elements of \mathcal{S}_M to zero). This produces a form where in each subsector, one of the quadratic powers is reduced by one, such that self-similarity to the original form cannot be generated anymore. In the course of the iterations, quadratic or higher powers will be generated unavoidably, such that a form which may lead to infinite recursion can occur at some point. In this case it has proven useful to choose, if existent, a set \mathcal{S} containing the maximal number of variables occurring with the *same* power. Certainly, these are only heuristic rules, which however worked well in a multitude of practical applications.

3.3 Examples

3.3.1 Planar double box with one off-shell leg

Two-loop box diagrams with one off-shell leg are master integrals entering for example the two-loop QCD matrix elements for $e^+e^- \rightarrow 3\text{jets}$ at NNLO [47]. Numerical results were first given in [16] and served as important benchmarks for the analytical calculations of Refs. [45, 46].

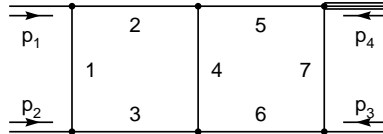


Figure 2: The planar double-box with leg 4 off-shell.

For the planar double box with $p_1^2 = p_2^2 = p_3^2 = 0, p_4^2 \neq 0$ shown in Fig. 2, the functions \mathcal{U} and \mathcal{F} are given by

$$\begin{aligned}
 \mathcal{U} &= x_{123}x_{567} + x_4x_{123567} \\
 \mathcal{F} &= (-s_{12})(x_2x_3x_{4567} + x_5x_6x_{1234} + x_2x_4x_6 + x_3x_4x_5) \\
 &\quad + (-s_{23})x_1x_4x_7 + (-p_4^2)x_7(x_2x_4 + x_5x_{1234}), \tag{24}
 \end{aligned}$$

where $x_{ijk\dots} = x_i + x_j + x_k + \dots$ and $s_{ij} = (p_i + p_j)^2$.

Iterated sector decomposition produces 197 sectors. As the off-shell leg regulates some of the singularities which would be present in the planar double box with all legs on-shell, the number of produced subsectors is lower than for the on-shell planar double box (282 subsectors). The result for two Euclidean points is given in Table 1, where an

overall factor of $\Gamma(1 + \epsilon)^2$ has been extracted and the integral is defined as⁴

$$\begin{aligned}
DB_{m4} &= \int \frac{d^D k_1}{i\pi^{\frac{D}{2}}} \int \frac{d^D k_2}{i\pi^{\frac{D}{2}}} \times \\
&\quad \frac{1}{k_1^2 k_2^2 (k_1 + p_1)^2 (k_1 + p_1 + p_2)^2 (k_2 + p_1 + p_2)^2 (k_2 - p_4)^2 (k_1 - k_2)^2} \\
&= \Gamma(1 + \epsilon)^2 \left(\frac{P_4}{\epsilon^4} + \frac{P_3}{\epsilon^3} + \frac{P_2}{\epsilon^2} + \frac{P_1}{\epsilon} + P_0 \right). \tag{25}
\end{aligned}$$

The computing time for the given precision, which is better than 0.3% for the finite

$(s_{12}, s_{23}, s_{13}, p_4^2)$	$(-1/3, -1/3, -1/3, -1)$	$(-1/2, -1/3, -1/6, -1)$
P_4	-26.9997 ± 0.00049	-11.9998 ± 0.0002
P_3	-118.651 ± 0.0037	-43.0010 ± 0.0027
P_2	-239.646 ± 0.0347	-58.6686 ± 0.0160
P_1	-305.823 ± 0.1835	-20.7692 ± 0.0560
P_0	-162.537 ± 0.435	$+98.191 \pm 0.289$

Table 1: Numerical results for the pole coefficients of the planar double-box with one leg off-shell. An overall prefactor of $\Gamma^2(1 + \epsilon)$ has been extracted.

part and better than 0.1% for the pole coefficients, was about 2 hrs on 3.0 GHz Intel Xeon processors. To obtain a precision of only 1% in the finite part takes about 30 minutes. The numerical evaluation has been done for each primary sector separately and the errors have been added in quadrature. The independent treatment of each primary sector allows to split the problem into smaller subparts which can be evaluated in parallel, such that the overall computing time is determined by the primary sector with the most complicated singularity structure. Further, symmetries of the diagram can serve as a check, as the results for the corresponding primary sectors should be identical. On the other hand, if large cancellations between different primary sectors are observed, summing over the primary sectors *before* the numerical integration is the better option.

3.3.2 Three-loop vertex diagram

As a more complicated example, let us consider the diagram shown in Fig. 3, entering the calculation of massless three-loop form factors [55]. It is given by

$$\begin{aligned}
A_8 &= \int \frac{d^D k_1}{(2\pi)^D} \int \frac{d^D k_2}{(2\pi)^D} \int \frac{d^D k_3}{(2\pi)^D} \times \\
&\quad \frac{1}{(k_1 + p_1)^2 k_2^2 k_3^2 (k_2 + p_1)^2 (k_1 + k_3)^2 (k_1 + k_3 + q)^2 (k_2 - k_1)^2 (k_2 + k_3)^2}, \tag{26}
\end{aligned}$$

where $q = p_1 + p_2$ is the incoming momentum, and again, an infinitesimal imaginary part $+i\delta$ in the propagators is understood. Iterated sector decomposition produced 684 sectors. The result is given in Table 2, where an overall prefactor of $i S_\Gamma^3 (-q^2 - i\delta)^{-2-3\epsilon}$

⁴An infinitesimal imaginary part $+i\delta$ in the propagators is understood, and we use $\mu = 1$.

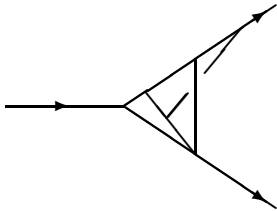


Figure 3: A non-planar 3-loop vertex diagram, called A_8 .

with $1/S_\Gamma = (4\pi)^{D/2} \Gamma(1 - \epsilon)$, has been extracted:

$$A_8 = iS_\Gamma^3 (-q^2 - i\delta)^{-2-3\epsilon} \left(\frac{P_2}{\epsilon^2} + \frac{P_1}{\epsilon} + P_0 + \epsilon P_\epsilon \right), \quad (27)$$

and the P_i are the coefficients given in Table 2. The computing time up to order ϵ was about 4 hrs on 3.0 GHz processors. Computing only the pole coefficients and the finite part took about 1 hour.

	numerical	analytic
P_2	3.20553 ± 0.00011	3.2054850751
P_1	8.42310 ± 0.00146	8.4222653365
P_0	27.885 ± 0.039	27.852843117
P_ϵ	-50.246 ± 0.129	-50.283167385

Table 2: Numerical results for the Laurent-expansion of the 3-loop vertex diagram shown in Fig. 3. The analytic result can be found in [55].

4 Sector decomposition for infrared divergent real radiation integrals

In order to calculate cross sections at higher orders in perturbation theory, there are in general not only virtual corrections, but also corrections from real radiation to be taken into account. At next-to-leading order, we only have two types of contributions: the purely virtual (one-loop) corrections, and the real radiation of one additional particle, which may be either theoretically or experimentally unresolved. “Theoretically unresolved” denotes the collinear branching of massless particles or the emission of soft photons or gluons, which leads to infrared singularities appearing as poles in $1/\epsilon$ in dimensional regularisation when integrated over the D -dimensional phase space. Experimentally unresolved particles do not lead to a $1/\epsilon$ -singularity. They are defined by a so-called “measurement function” defining the physical observable, which in most cases is a subroutine in a numerical program rather than an analytic function. For example, two particles which are clustered into a single jet by a certain jet algorithm are considered as experimentally unresolved.

At NNLO, one generally has to deal with three building blocks making up the full cross section: two-loop (and one-loop squared) virtual corrections, one-loop virtual cor-

rections combined with single unresolved real radiation, and doubly unresolved real radiation.

As any D -dimensional phase space integral can be transformed to a dimensionally regulated multi-parameter integral over the unit hypercube, the singularities stemming from the (theoretically) unresolved real radiation are amenable to sector decomposition applied to phase space integrals over the corresponding squared matrix elements. What matters here are the *denominators* of the matrix elements for different processes, which have a generic form, and therefore allow for the setup of a general framework.

4.1 Phase space integrals in D dimensions

The phase space integral in D dimensions for a generic process $Q \rightarrow p_1 + \dots + p_N$ can be written as

$$\int d\Phi_N^D = (2\pi)^{N-D(N-1)} \int \prod_{j=1}^N d^D p_j \delta^+(p_j^2 - m_j^2) \delta^{(D)}\left(Q - \sum_{i=1}^N p_i\right), \quad (28)$$

where $\delta^+(p^2 - m^2) = \delta(p^2 - m^2)\Theta(p^0)$. Using

$$\int d^D p_j \delta^+(p_j^2 - m_j^2) = \frac{1}{2E_j} \int d^{D-1} \vec{p}_j \Big|_{E_j = \sqrt{\vec{p}_j^2 + m_j^2}}$$

for $j = 1, \dots, N-1$ and eliminating p_N by momentum conservation, one obtains

$$\int d\Phi_N^D = \frac{(2\pi)^{N-D(N-1)}}{2^{N-1}} \int \prod_{j=1}^{N-1} d^{D-1} \vec{p}_j \frac{\Theta(E_j)}{E_j} \delta^+\left(\left(Q - \sum_{i=1}^{N-1} p_i\right)^2 - m_N^2\right) \Big|_{E_j = \sqrt{\vec{p}_j^2 + m_j^2}}.$$

To proceed, one has to choose a certain parametrisation for the phase space integration variables and work out the integration limits confining the integration range to the physical region. The scattering case $Q = p_a + p_b \rightarrow N-1$ particles differs from a decay $1 \rightarrow N$ particles by the fact that in the center-of-mass frame of the incident particles, it contains a preferred direction given by the beam axis $\vec{p}_a = -\vec{p}_b$. Finding the appropriate phase space integration variables which are optimally adapted to the kinematic situation at hand can simplify the calculation considerably. This is even more true if sector decomposition is used to isolate the infrared singularities: a convenient parametrisation will be one where the maximal number of potentially singular denominators of the matrix element naturally factorises, thus limiting the number of terms produced by iterated decompositions. In fact, it turns out to be useful to divide the matrix element into different “topologies”, according to their denominator structure, and use several phase space parametrisations, each being optimal for a certain class of topologies.

A multi-particle phase space is most conveniently described as a convolution of phase spaces of lower multiplicity. For example, a process like the one in Fig. 4 suggests a phase space parametrisation which is a convolution of a phase space for a $1 \rightarrow 4$ decay followed by a $1 \rightarrow 3$ decay and a $1 \rightarrow 2$ splitting. For a process involving soft radiation off massive fermions, it is convenient to choose a parametrisation where the energy of the particle which can become soft is an integration variable. Useful examples of different parametrisations can be found e.g. in [28, 83, 84]. Here, in order to illustrate some generic features of the method, we will first derive a phase space parametrisation in terms of double invariants $s_{ij} = (p_i + p_j)^2$.

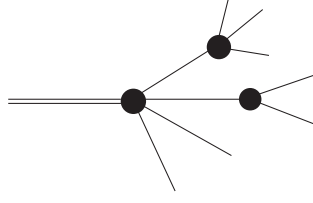


Figure 4: Example of a cascade decay corresponding to an iterative construction of a multi-particle phase space.

As a pedagogical example we will consider the massless case, $p_j^2 = 0$. Let us choose a $1 \rightarrow 4$ process and consider a special frame where

$$\begin{aligned}
Q &= (E, \vec{0}^{(D-1)}) \\
p_1 &= E_1 (1, \vec{0}^{(D-2)}, 1) \\
p_2 &= E_2 (1, \vec{0}^{(D-3)}, \sin \theta_1, \cos \theta_1) \\
p_3 &= E_3 (1, \vec{0}^{(D-4)}, \sin \theta_2 \sin \theta_3, \sin \theta_2 \cos \theta_3, \cos \theta_2) \\
p_4 &= Q - p_1 - p_2 - p_3,
\end{aligned} \tag{29}$$

which leads to

$$\begin{aligned}
d\Phi_{1 \rightarrow 4} &= \frac{1}{8} (2\pi)^{4-3D} dE_1 dE_2 dE_3 d\theta_1 d\theta_2 d\theta_3 [E_1 E_2 E_3 \sin \theta_1 \sin \theta_2]^{D-3} \sin \theta_3^{D-4} \\
&\quad d\Omega_{D-2} d\Omega_{D-3} d\Omega_{D-4} \Theta(E_1) \Theta(E_2) \Theta(E_3) \Theta(E - E_1 - E_2 - E_3) \\
&\quad \delta(E^2 - 2E(E_1 + E_2 + E_3) + 2(p_1 \cdot p_2 + p_1 \cdot p_3 + p_2 \cdot p_3)), \tag{30}
\end{aligned}$$

where

$$\int d\Omega_{D-1} = \int_0^{2\pi} d\theta_1 \int_0^\pi d\theta_2 \sin \theta_2 \dots \int_0^\pi d\theta_{D-1} (\sin \theta_{D-1})^{D-2} = \frac{2\pi^{\frac{D}{2}}}{\Gamma(\frac{D}{2})}.$$

Now we map the angle and energy variables to the double invariants s_{ij} as integration variables, using the Jacobian

$$\det(J) = \det \left(\frac{\partial(s_{..})}{\partial(E_i, \theta_j)} \right) = 64 E^3 E_1^2 E_2^2 E_3^2 \sin \theta_1^2 \sin \theta_2^2 \sin \theta_3. \tag{31}$$

The Jacobian in combination with terms already present in (30) can be written as the determinant Δ_4 of the Gram matrix $G_{ij} = 2 p_i \cdot p_j$. This determinant can be expressed by the Källén function $\lambda(x, y, z) = x^2 + y^2 + z^2 - 2xy - 2yz - 2xz$ as

$$\Delta_4 = \lambda(s_{12} s_{34}, s_{13} s_{24}, s_{14} s_{23}) = -(4 E E_1 E_2 E_3 \sin \theta_1 \sin \theta_2 \sin \theta_3)^2. \tag{32}$$

We see that Δ_4 has to be negative semi-definite. With the dimensionless variables

$$y_1 = s_{12}/Q^2, y_2 = s_{13}/Q^2, y_3 = s_{23}/Q^2, y_4 = s_{14}/Q^2, y_5 = s_{24}/Q^2, y_6 = s_{34}/Q^2 \tag{33}$$

and $\hat{\Delta}_4 = \lambda(y_1 y_6, y_2 y_5, y_3 y_4)$ we obtain finally

$$d\Phi_{1 \rightarrow 4} = (2\pi)^{4-3D} (Q^2)^{3D/2-4} 2^{-2D+1} d\Omega_{D-2} d\Omega_{D-3} d\Omega_{D-4} \left[\prod_{j=1}^6 dy_j \Theta(y_j) \right] \Theta(-\hat{\Delta}_4) [-\hat{\Delta}_4]^{(D-5)/2} \delta(1 - \sum_{j=1}^6 y_j). \quad (34)$$

For $N \geq 5$ we have to distinguish if we are in D dimensions or in four dimensions. In D dimensions, the same procedure as above can in principle be applied. The four-dimensional case is complicated by the fact that the Gram determinant Δ_N vanishes for $N > 4$. In this case the phase space can be expressed in terms of the Källén function of invariants built from four independent momenta and additional constraints [83], but in practice it is more useful to build it up iteratively as described above.

4.2 Special features of sector decomposition for real radiation

We see that expression (34) has a high symmetry in the invariants y_j . To proceed in a way analogous to the treatment of loop integrals, we could now do a “primary sector decomposition” to integrate out the δ -function as explained in section 3.2. This would lead to n primary sectors, where n is the number of two-particle invariants s_{ij} , i.e. $n = 6$ in the example above. All invariants are treated on equal footing in this step. The primary sector decomposition is very useful in the case of loop integrals, mainly for the following reason: it preserves the feature that singularities *only* occur at special *points* at the boundary of parameter space: they occur only if $y_{i_1}, \dots, y_{i_r} = 0$ for a subset $\{i_1 \dots i_r\}$ of $\{1 \dots n\}$. In other words, in the case of loop integrals in the Euclidean region, no singularities can occur for $y_i \rightarrow 1$ or in the interior of parameter space, and by primary sector decomposition the δ -constraint is integrated out without destroying this feature. In addition, the integration limits from zero to one for all remaining variables are guaranteed without further transformations.

In the case of real radiation, the situation is different, because we are forced to stay within the physically allowed region. In the parametrisation above, this is reflected by the fact that after integrating out the constraint $\delta(1 - \sum_{i=1}^n y_i)$ from momentum conservation, we still have the constraint $\Theta(-\Delta_4)$. Solving the equation $\Delta_4 = 0$ for say, y_k , we obtain the solution $y_k^\pm = (\sqrt{x} \pm \sqrt{z})^2$, so $y_k^- = 0$ whenever $x = z$. For example, for $k = 3$, we have

$$y_3^\pm = (\sqrt{y_2 y_5} \pm \sqrt{y_1 y_6})^2 / y_4. \quad (35)$$

The substitution $y_3 = y_3^- + t_3 (y_3^+ - y_3^-)$ in order to remap all integrations to the unit interval will lead to a complicated structure of those denominators in the matrix element which contain y_3 . In fact, we see that $1/y_3$ will develop a singularity if $t_3 = 0$ and y_3^- simultaneously, i.e. whenever $t_3 = 0$ and $y_2 y_5 = y_1 y_6$. Thus we found two properties which did not occur in the case of loop integrals:

1. Square-root terms appear naturally when solving the phase space constraints. Such terms are potentially dangerous as they may destroy the polynomial structure which is a prerequisite for the sector decomposition, leading to expressions like $g(x, y) = a + y - \sqrt{a^2 + x^2}$, where a is a constant. However, it is obvious that such terms can be easily transformed into a form with the required behaviour under rescaling of the variables.

2. After having mapped the phase space integration limits to the unit hypercube, singularities can occur for a *manifold* which (partly) lies *inside* the phase space integration region.

How these singularities can be remapped to the boundaries will be shown in a specific example below and discussed more generally in Section 4.4. Here we would like to point out that we cannot solve the constraint $\Theta(-\Delta_4)$ for the same variable y_k in each primary sector, because in primary sector k , y_k has been eliminated. Therefore a judicious choice of y_k — to be an invariant which occurs only in very few or no denominators of the complete matrix element — would still lead to complicated denominators in primary sector k , where the constraint had to be solved for $y_{i \neq k}$. For this reason it is advisable not to use primary sector decomposition in the case of complicated matrix elements for real radiation.

	loop integrals	phase space integrals
parametrisation	\mathcal{F}, \mathcal{U} functions in terms of Feynman parameters fixed	many different options, should be adapted to topologies
primary sector dec.	very convenient	not recommended
singularity structure	in Euclidean region only endpoint singularities	singularities inside integration region generic

Table 3: Main differences to loop integrals in the sector decomposition procedure for phase space integrals over IR divergent real radiation

To choose a parametrisation which is adapted to the denominator structure of the problem, one can follow the idea of iterative splittings outlined above. Matrix elements involving massless particles contain invariants of the form $s_{i_1 \dots i_n} = (p_{i_1} + \dots + p_{i_n})^2$ with $n \geq 2$ in the denominator. For example, the four-particle cut of the diagram in Fig. 5

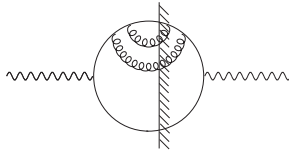


Figure 5: Example of a four-particle cut.

contains an integral of the form [23]

$$J_4 = \frac{4}{\pi} \int_0^\infty \prod_{i=1}^6 dy_i \Theta(-\Delta_4) (-\Delta_4)^{-1/2-\epsilon} \delta\left(1 - \sum_{j=1}^6 y_j\right) \frac{(y_1 + y_5)(y_2 + y_6) - y_3 y_4}{y_2 (y_2 + y_4 + y_6)^2}. \quad (36)$$

In this case, it is suggestive to introduce the triple invariant $s_{134}/Q^2 = y_2 + y_4 + y_6$ as

a genuine phase space variable, such that this denominator factorises immediately. This example will be worked out in detail in the following section.

Obviously, it is advantageous to use triple invariants as phase space integration variables if the amplitude contains a splitting of one particle into three final state particles, double invariants if the amplitude contains several $1 \rightarrow 2$ splittings, etc. Therefore the choice of parametrisation is most conveniently done on a topology basis, i.e. different parametrisations are applied to certain classes of denominator structures, as already mentioned above. As the full matrix element contains interferences of amplitudes of different “splitting history”, it is in general impossible to achieve a factorised form for *all* denominators. However, minimising the number of decompositions by convenient parametrisations is vital to limit the size of the expressions produced by iterated sector decomposition.

The main differences to loop integrals in the sector decomposition procedure for phase space integrals are again summarised in Table 3.

4.3 Example of a four-particle final state

To explain the concept, we go back to the example of the previous section, the massless $1 \rightarrow 4$ phase space, and topologies containing s_{134} or s_{234} in the denominator. In order to achieve a convenient parametrisation, we first multiply eq. (34) by

$$1 = \int dx_4 \delta(x_4 - y_2 - y_4 - y_6) \int dx_5 \delta(x_5 - y_3 - y_5 - y_6)$$

and eliminate y_1, y_4, y_5 using the δ -functions (see eq. (33) for the definition of the scaled invariants). Then we solve the constraint $(-\Delta_4) \geq 0$ for $y_3 = s_{23}/Q^2$ and substitute $y_3 \rightarrow y_3^- + t_3(y_3^+ - y_3^-)$. For the remaining variables we substitute

$$\begin{aligned} x_4 &= t_4 \\ x_5 &= t_1 + t_5(1 - t_1)(1 - t_4) \\ y_2 &= t_1(1 - t_2)t_4 \\ y_6 &= t_1 t_4 \end{aligned} \tag{37}$$

to arrive at the following form for the phase space

$$\begin{aligned} \int d\Phi_{1 \rightarrow 4} &= (2\pi)^{4-3D} (Q^2)^{3D/2-4} 2^{-2D+1} d\Omega_{D-2} d\Omega_{D-3} d\Omega_{D-4} \\ &\int_0^1 dt_1 \dots dt_5 [(1 - t_1)t_4(1 - t_4)]^{D-3} [t_1 t_2(1 - t_2)t_5(1 - t_5)]^{\frac{D-4}{2}} [t_3(1 - t_3)]^{(D-5)/2}. \end{aligned} \tag{38}$$

The expression for J_4 in eq. (36) then becomes

$$\begin{aligned} J_4 &= \frac{4}{\pi} \int_0^1 dt_1 \dots dt_5 [t_1(1 - t_2)]^{-1-\epsilon} t_4^{-1-2\epsilon} (1 - t_1)^{1-2\epsilon} (1 - t_4)^{2-2\epsilon} \\ &\quad [t_2 t_5(1 - t_5)]^{-\epsilon} [t_3(1 - t_3)]^{-1/2-\epsilon} ((t_1(1 - t_2) + t_2) - \tilde{y}_3(\vec{t})) \\ \tilde{y}_3(\vec{t}) &= t_2 t_5 + t_1(1 - t_2)(1 - t_5) - 2(1 - 2t_3) \sqrt{t_1 t_2 t_5(1 - t_2)(1 - t_5)} \\ &= y_3(\vec{t})/(1 - t_4). \end{aligned} \tag{39}$$

We see that in this parametrisation, the denominators in J_4 are factorising completely. However, other denominators in the full matrix element will in general contain $\tilde{y}_3(\vec{t})$ in the denominator. In this case it is convenient to shuffle the square-root terms to the numerator by the following non-linear transformation [22]: We substitute

$$t_3 = \frac{y_3^-(1-z_3)}{y_3^- + z_3(y_3^+ - y_3^-)} \Rightarrow y_3 = \frac{y_3^+ y_3^-}{y_3^- + z_3(y_3^+ - y_3^-)}. \quad (40)$$

The Jacobian therefore cancels one factor of y_3 in the denominator:

$$\frac{dt_3}{dz_3} = \frac{y_3^+ y_3^-}{[y_3^- + z_3(y_3^+ - y_3^-)]^2} = \frac{y_3}{y_3^- + z_3(y_3^+ - y_3^-)}, \quad (41)$$

leading to

$$\begin{aligned} & \int_0^1 dt_3 [t_3(1-t_3)]^{\frac{D-5}{2}} \frac{1}{y_3(\vec{t})} = \int_0^1 dt_3 [t_3(1-t_3)]^{\frac{D-5}{2}} \frac{1}{y_3^- + t_3(y_3^+ - y_3^-)} \\ & = \int_0^1 dz_3 [z_3(1-z_3) y_3^+ y_3^-]^{\frac{D-5}{2}} [y_3^- + z_3(y_3^+ - y_3^-)]^{4-D}. \end{aligned} \quad (42)$$

This way the square-roots in the denominator are eliminated and the limits $t_3 \rightarrow 0$ and $y_3^- \rightarrow 0$ are decoupled, but note that instead of $1/y_3(\vec{t})$ we now have a factor

$$[y_3^+ y_3^-]^{\frac{D-5}{2}} = [(1-t_4)(t_1(1-t_2)(1-t_5) - t_2 t_5)]^{D-5} = (1-t_4)^{D-5} [f(t_1, t_2, t_5)]^{D-5}.$$

The factor $(1-t_4)^{D-5}$ will be combined with phase space factors and is of endpoint-type anyway, but there are singularities which now occur on a manifold defined by $f(t_1, t_2, t_5) = 0$. In the case at hand they are easily remapped to the boundaries by splitting e.g. the t_2 -integration region at

$$t_2^0 = \frac{t_1(1-t_5)}{t_5 + t_1(1-t_5)} \quad (43)$$

and substituting

$$\begin{aligned} t_2 &= t_2^0 u_2 & \text{for } t_2 < t_2^0, \\ t_2 &= 1 - (1 - t_2^0) u_2 & \text{for } t_2 > t_2^0 \end{aligned} \quad (44)$$

to obtain again integrals from zero to one.

4.4 Possible types of singularities and their treatment

As we have seen in the previous section, we have to deal with the following types of singularities:

- endpoint singularities
- singularities on a manifold not confined to the boundaries of phase space, more precisely the boundaries after having solved all constraints and remapped the integrations to the unit hypercube.

Endpoint singularities, if not factorising from the start, are easily extracted by the sector decomposition algorithm. It should be mentioned however that, if we do not use primary sector decomposition, endpoint singularities can occur not only if an integration variable goes to zero, but also at the upper integration boundary (which is equal to one, after appropriate remapping). In order to apply the algorithm described in section 3.2, we should remap the singularities for $t_k \rightarrow 1$ such that they occur at the origin only. As some variables can cause singularities at zero *and* one, a transformation $t_k \rightarrow 1 - t_k$ is not recommended. Instead, we split the integration range at $1/2$: After the split

$$\int_0^1 dt_k = \underbrace{\int_0^{\frac{1}{2}} dt_k}_{(a)} + \underbrace{\int_{\frac{1}{2}}^1 dt_k}_{(b)}$$

and the substitution $t_k = u_k/2$ in (a) and $t_k = 1 - u_k/2$ in (b), all endpoint singularities occur at $u_k \rightarrow 0$ only. The disadvantage of such splittings is the fact that we end up with 2^n integrals after n splittings, but in practice, considering the physically possible singular limits, some of the integration variables clearly never will lead to a singularity when approaching one, and therefore do not require such a splitting.

Concerning the singularities at the interior of phase space, the recipe is less simple. However, for $N < 5$ in a $1 \rightarrow N$ or a $2 \rightarrow N - 1$ phase space, it is easy to see that they can always be remapped to the phase space boundaries. Quite in general, the boundaries of the physical region in the space of invariants follow from the momentum conserving δ -function and the Gram determinants $\Delta_N = \Delta(p_1, \dots, p_N) = \det(p_i \cdot p_j)$. As the Gram matrices are symmetric, the determinants will be polynomials of maximal degree two in each invariant s_{ij} . Masses do not alter this argument, and one can show that always $\Delta_3 \geq 0$ and $\Delta_4 \leq 0$ [84]. The case $N = 3$ is trivial, so let us first consider the case $N = 4$. Solving the constraint $\Theta(-\Delta_4)$ for one of the invariants y_k leads to $y_k^\pm = (\sqrt{a_k} \pm \sqrt{b_k})^2 / c_k$, where the structure of a_k, b_k, c_k is fixed by the fact that $\Delta_4 \leq 0$ is a Källén function: these terms must be *linear* in each invariant (see e.g. eq. (35)). After having performed substitutions of the type (37) to eliminate the momentum conserving δ -function, the linearity is not manifestly preserved, but as the singularity structure cannot change by these substitutions, some of the t_i must always factorise, which guarantees that the condition $\Delta_4 \leq 0$ imposing the phase space boundaries in the new variables can be solved for, say, the variable t_j^0 in such a way that t_j^0 is the ratio of two polynomials in the remaining parameters (see e.g. eq. (43)), therefore leading to structures amenable to sector decomposition.

For $N \geq 5$, in a $1 \rightarrow N$ or a $2 \rightarrow N - 1$ phase space, additional constraints are present due the fact that, for 4-dimensional momenta, $\Delta_N = 0$ for $N \geq 5$. However, if the phase space is expressed in terms of a convolution of processes of lower multiplicity as explained above, the same reasoning for the remapping of singularities as in the $N < 5$ case can be applied.

Different phase space parametrisations are related by Lorentz transformations, therefore it is sufficient to show this property for a particular parametrisation. This does not mean that all parametrisations actually do have the desired properties, it only states that a better parametrisation must exist where the remapping to a form more suitable for sector decomposition is possible.

One last point concerning different types of singularities should be made: In renormalisable theories, the “physical” singularities are not worse than logarithmic, which means that the parameter integrals after sector decomposition should be of the form $\int_0^1 dx x^{a+b\epsilon} f(x)$, where $a \geq -1$. If only the denominators are considered in a complex matrix element, terms with $a < -1$ will occur. This type of spurious singularity will finally cancel with terms from the numerator, but the cancellation is not manifest if we leave the numerator symbolic throughout the whole procedure. Therefore it is advisable to include the numerator at the level of the ϵ -expansion, at least for the parts where $a < -1$.

4.5 Construction of a differential Monte Carlo program

The isolation of infrared poles by sector decomposition is an algebraic procedure, leading to a set of finite functions for each pole coefficient as well as for the finite part. The finite functions have the form of parameter integrals over the unit interval and are therefore well suited for integration by Monte Carlo methods. If a full cross section beyond the leading order, composed of both real and virtual corrections, is to be calculated, the combination of the sector decomposition approach for the real radiation part with analytic results (if available) for the part involving loop corrections is certainly possible. In the case of NNLO corrections, it is also advisable, as the fully numerical evaluation of two-loop integrals in combination with the phase space integration is in general rather slow, if viable at all. However, at NLO, examples of a fully numerical evaluation of complete processes based on the combination of sector decomposition with contour deformation do exist [58, 59].

A hybrid approach can consist for example in the reduction of the phase space integrals to cut master integrals, evaluating only the master integrals by sector decomposition [21]. Concerning the mixed one-loop times single unresolved real radiation part of NNLO calculations, its treatment so far always involved a reduction to master integrals [24, 28, 29], except in the very recent calculation of the $O(\alpha_s^2)$ corrections to semileptonic decay $b \rightarrow c l \bar{\nu}_l$ [41]. For these mixed real-virtual contributions, it can further be useful to do parts of the Feynman parameter integrations for the master integrals analytically, to obtain Hypergeometric functions where transformation formulas for the arguments [85, 86] can be used if necessary to arrive at a more convenient form. Then one can proceed by applying sector decomposition to the integral representation of the Hypergeometric functions in combination with the phase space variables [29, 87].

To obtain differential results, the combination of the output of the sector decomposition procedure with any infrared safe measurement function is possible, as has been first noted in [22]. The flexibility to do so is achieved by expanding the singular factors produced by the decomposition into plus-distributions, using the identity

$$x^{-1+\kappa\epsilon} = \frac{1}{\kappa\epsilon} \delta(x) + \sum_{n=0}^{\infty} \frac{(\kappa\epsilon)^n}{n!} \left[\frac{\ln^n(x)}{x} \right]_+,$$

where

$$\int_0^1 dx f(x) [g(x)/x]_+ = \int_0^1 dx \frac{f(x) - f(0)}{x} g(x). \quad (45)$$

This is basically equivalent to the ϵ -expanded form of eq. (21), the only difference being that, instead of integrating out the singular factors explicitly, the integrands are kept in

the form of distributions: $\int_0^1 dx x^{-1+\kappa\epsilon} f(0, y)$ is written as $\int_0^1 dx \frac{1}{\kappa\epsilon} \delta(x) f(x, y)$ instead of $\frac{1}{\kappa\epsilon} f(0, y)$. This allows for the combination with arbitrary functions $f(x, y)$.

The following features which are special to the sector decomposition approach as compared to Monte Carlo programs based on analytic subtraction terms should be pointed out:

- The pole coefficients are only calculated numerically, such that the cancellation of poles between real, real-virtual (existing beyond NLO only) and purely virtual contributions can be verified only numerically. However, this is in general not a problem because the pole coefficients contain less integration variables and therefore a high numerical precision can be achieved more easily than for the finite part.
- The expansion into plus distributions cannot be done in complete isolation from the measurement function, because it has to be assured that the subtraction terms only come to action in phase space regions which are allowed by the measurement function. To illustrate this point, consider the simple one-dimensional example where the measurement function is just a step function $\Theta(x - a)$, $a > 0$, and the “matrix element” after sector decomposition is given by $f(x)$. If we expand into plus distributions and *afterwards* just multiply with our measurement function, we obtain

$$\int_0^1 dx \frac{f(x) - f(0)}{x} \Theta(x - a) = f(0) \ln a + \int_a^1 dx \frac{f(x)}{x}. \quad (46)$$

Clearly, the $f(0)$ term stems from the subtraction of a singularity at $x = 0$, which is now killed by our measurement function anyway, such that inclusion of the $f(0)$ term would lead to a wrong result. The correct way is of course to include the measurement function into the expression the plus distribution acts on. However, this does *not* mean that the ϵ -expansions and subtractions have to be redone each time the measurement function is changed. It can be achieved by including symbolic functions in the ϵ -expansion which are written to the numerical code with zero arguments (respectively the appropriate singular limit in the general case) if they correspond to subtraction terms. The symbolic functions can be specified later in a subroutine of the numerical program.

- The subroutines defining jets, observables etc. will be based on the four-momenta of the particles involved in the scattering process. The four-momenta can easily be constructed from the *original* phase space integration variables. Before the decomposition, the phase space integration variables, let us call them s_{ij} , have a certain functional form, $s_{ij} = s_{ij}(t_1, \dots, t_n)$. Performing now iterated sector decomposition will remap the parameters t_i , in a different way in each subsector of the decomposition tree, such that *after* iterated sector decomposition, the functional dependence of the original variables on the Monte Carlo integration parameters t_1, \dots, t_n is different for each subsector. Of course it is easy to keep track of the remappings done in each sector, but the Monte Carlo program will consist of a sum of contributions from each subsector k , each one defining the functional form $s_{ij}^{(k)}(t_1, \dots, t_n)$ in a different way. This is not a problem in principle, but the complexity of NNLO matrix elements is already enormous, so multiplying the evaluation time by the number of subsectors, which is of the order of several hundreds for an NNLO process, can lead to unacceptable CPU times.

- As the subtractions done after sector decomposition are of the form

$$\int_0^1 dx \frac{f(x) - f(0)}{x}$$

in each variable, which means that poles in each variable are *locally* subtracted, the method in general leads to expressions which have a good numerical behaviour. In fact, as even integrable singularities of the type $\int_0^1 dx dy \frac{1}{x+y}$ are decomposed, the expressions produced by iterated sector decomposition are of a form which is very convenient for numerical integrations. However, if the matrix elements to evaluate exceed a certain degree of complexity, there is a turnover where the advantage gained from the form of the individual functions is destroyed by the sheer number of functions to evaluate. This has been found for example in the attempt to calculate the full real corrections for $e^+e^- \rightarrow 3$ jets at NNLO using only sector decomposition. The calculation of this process has recently been accomplished [88–91] using analytic “antenna” subtraction [92]. Due to the large number of massless particles, the infrared structure is extremely complicated, and the number of antenna subtraction terms needed for the analytic subtraction of the poles is already quite large. Using sector decomposition leads to an unacceptable number of terms in this case. On the other hand, if massive particles are involved, the situation is completely different: while analytic integrations of subtraction terms become nearly impossible for NNLO calculations with several mass scales, the infrared singularity structure is less complex in the presence of masses, such that the number of terms produced by sector decomposition will be moderate, and the mass dependence of the finite terms produced by the decomposition does not pose a problem for the numerical integration.

5 Conclusions and outlook

The method of sector decomposition is interesting from a more formal field theoretical point of view as well as for phenomenological applications. Within the context of dimensional regularisation, it offers a *constructive* scheme for the factorisation and subtraction of infrared poles to (in principle) all orders in perturbation theory, not only for individual integrals, but also for entire squared matrix elements.

Quite in general, the method consists of two parts: the first is an algebraic one, where the singularities are isolated in terms of a Laurent series in ϵ , the coefficients being finite parameter integrals. The second part consists in the evaluation of these parameter integrals, which in general is not possible analytically, and is therefore done numerically by Monte Carlo integration. Obviously the precision which can be achieved this way is intrinsically limited, compared to the evaluation of functions where all integrations have been performed analytically, or where deterministic numerical integration methods can be applied. However, in most practical applications considered so far, sufficient precision could be reached within a reasonable amount of integration time.

Applications of the method to multi-loop integrals have been very successful in providing predictions and cross-checks for cutting-edge analytical calculations, e.g. various types of two-loop box integrals or three-loop vertex functions. A restriction of the method for multi-loop integrals presented here is given by the fact the numerical evaluation is straightforward only for Euclidean points, where all kinematic invariants are negative.

For one-scale problems, like massless two-point or three-point functions, this is not a restriction at all, but if more than three external legs or/and masses are present, there will be branch cuts and thresholds which hinder a straightforward numerical evaluation. Solutions to this problem already have been suggested [32, 41, 42, 58, 59, 62, 64] and are subject to current research.

Although the algorithm is valid to all orders in principle, there are certainly limitations from CPU-time and memory once a certain degree of complexity is reached. It is not possible to make a general statement about where exactly the limit is, as it depends not only on the computing resources but also on the way the algorithm is programmed. Further, the number of loops and scales is not the only measure of complexity. Non-planar diagrams in general lead to more complicated expressions, often containing spurious singularities with worse than logarithmic behaviour at intermediate stages.

In combination with its application to infrared singular real radiation, the method of sector decomposition has proven very useful recently to obtain differential results for full processes at NNLO [24, 26, 28, 29, 31, 38, 41]. The main advantages compared to methods based on analytic subtraction are the following: the subtraction procedure lends itself to automation and, due to the “local” nature of the subtraction terms, leads to expressions with good numerical behaviour. There is no need for an analytic integration of subtraction terms over the singular phase space regions, which is a big advantage in the presence of massive particles. The main drawback of the method consists in the fact that it leads to very large expressions for complex processes, as the number of terms is increased in each decomposition step. In particular for processes involving many massless particles, necessitating a large number of subtraction terms, like e.g. $e^+e^- \rightarrow 3\text{jets}$ or $pp \rightarrow 2\text{jets}$ at NNLO, the size of the expressions produced by sector decomposition reaches a limit where differential results with sufficient numerical precision cannot be obtained within reasonable CPU times. Fortunately, most processes relevant for high precision phenomenology involve both massive and massless particles, where the method of sector decomposition has an enormous potential, not suffering from the limitations imposed by analytic integrability.

Part of the problem with intractably large expressions is related to the fact that the algorithm, in its fully automated form, makes a decomposition already if the *necessary* condition to produce a singularity in $1/\epsilon$ is fulfilled (e.g. vanishing of the function \mathcal{F} in the case of loop integrals). However, this is not always *sufficient* to produce a singularity. Knowledge about the physical singularity structure (i.e. the soft and collinear limits) and inspection by eye of certain terms can certainly help to prevent unnecessary decompositions, but the applicability of such criteria is rather limited for complicated expressions as occurring e.g. in NNLO matrix elements, where a fully automated treatment is mandatory. Therefore, in order to minimise the number of produced terms, it would be useful to have an algorithm which finds the *minimal* number of decompositions necessary to extract the singularities. In the case of scalar loop integrals, this is basically a mathematical problem. If full processes are considered, a solution depends crucially on the way the numerator functions are treated. In any case this issue deserves further study.

Finally, it is clear that the key to an optimal solution often consists in combining several methods in a clever way. The universality of sector decomposition, as a general method to isolate singularities from parameter integrals, suggests that it is a good candidate for such combined approaches.

Acknowledgements

I would like to thank T. Binoth for fruitful collaboration on the subject, especially in what concerns the algorithm for multi-loop integrals. I am also very grateful to V. A. Smirnov for providing analytic challenges of always increasing complexity allowing to test my program, and for continuous encouragement. I also would like to thank A. Gehrmann-DeRidder and T. Gehrmann for useful comparisons and encouragement concerning the application to phase space integrals. Further, I am grateful to T. Binoth, M. Czakon, T. Gehrmann and V. A. Smirnov for comments on the manuscript. This research was supported by the UK Science and Technology Facilities Council.

References

- [1] N. N. Bogoliubov and O. S. Parasiuk, *On the multiplication of the causal function in the quantum theory of fields*, *Acta Math.* **97** (1957) 227–266.
- [2] K. Hepp, *Proof of the Bogolyubov-Parasiuk theorem on renormalization*, *Commun. Math. Phys.* **2** (1966) 301–326.
- [3] W. Zimmermann, *Convergence of Bogolyubov’s method of renormalization in momentum space*, *Commun. Math. Phys.* **15** (1969) 208–234.
- [4] T. Kinoshita, *Mass singularities of Feynman amplitudes*, *J. Math. Phys.* **3** (1962) 650–677.
- [5] T. D. Lee and M. Nauenberg, *Degenerate systems and mass singularities*, *Phys. Rev.* **133** (1964) B1549–B1562.
- [6] K. Pohlmeier, *Large Momentum Behavior of the Feynman Amplitudes in the ϕ^4 in Four-Dimensions Theory*, *J. Math. Phys.* **23** (1982) 2511.
- [7] P. Breitenlohner and D. Maison, *Dimensionally Renormalized Green’s Functions for Theories with Massless Particles. 1*, *Commun. Math. Phys.* **52** (1977) 39.
- [8] P. Breitenlohner and D. Maison, *Dimensionally Renormalized Green’s Functions for Theories with Massless Particles. 2*, *Commun. Math. Phys.* **52** (1977) 55.
- [9] E. R. Speer, *Ultraviolet and infrared singularity structure of generic Feynman amplitudes*, *Annales Poincare Phys. Theor.* **23** (1975) 1–21.
- [10] E. R. Speer, *Mass Singularities of Generic Feynman Amplitudes*, *Annales Poincare Phys. Theor.* **26** (1977) 87–105.
- [11] K. G. Chetyrkin and F. V. Tkachov, *Infrared R Operation and Ultraviolet counterterms in the MS Scheme*, *Phys. Lett.* **B114** (1982) 340–344.
- [12] K. G. Chetyrkin and V. A. Smirnov, *R* Operation Corrected*, *Phys. Lett.* **B144** (1984) 419–424.
- [13] V. A. Smirnov, *Renormalization and asymptotic expansions*. Birkhaeuser (Progress in physics 14, 380 p.) Basel, Switzerland, 1991.

- [14] V. A. Smirnov, *Evaluating Feynman integrals*, Springer Tracts Mod. Phys. **211** (2004) 1–244.
- [15] M. Roth and A. Denner, *High-energy approximation of one-loop Feynman integrals*, Nucl. Phys. **B479** (1996) 495–514, [hep-ph/9605420].
- [16] T. Binoth and G. Heinrich, *An automatized algorithm to compute infrared divergent multi-loop integrals*, Nucl. Phys. **B585** (2000) 741–759, [hep-ph/0004013].
- [17] G. Heinrich, *et al*, *a public version is in preparation*.
- [18] C. Bogner and S. Weinzierl, *Comput. Phys. Commun.* **178** (2008) 596 [hep-ph/0709.4092].
- [19] G. 't Hooft and M. J. G. Veltman, *Regularization and Renormalization of Gauge Fields*, Nucl. Phys. **B44** (1972) 189–213.
- [20] C. G. Bollini and J. J. Giambiagi, *Dimensional Renormalization: The Number of Dimensions as a Regularizing Parameter*, Nuovo Cim. **B12** (1972) 20–25.
- [21] A. Gehrmann-De Ridder, T. Gehrmann, and G. Heinrich, *Four-particle phase space integrals in massless QCD*, Nucl. Phys. **B682** (2004) 265–288, [hep-ph/0311276].
- [22] C. Anastasiou, K. Melnikov, and F. Petriello, *A new method for real radiation at NNLO*, Phys. Rev. **D69** (2004) 076010, [hep-ph/0311311].
- [23] T. Binoth and G. Heinrich, *Numerical evaluation of phase space integrals by sector decomposition*, Nucl. Phys. **B693** (2004) 134–148, [hep-ph/0402265].
- [24] C. Anastasiou, K. Melnikov, and F. Petriello, *Real radiation at NNLO: $e^+e^- \rightarrow 2$ jets through $O(\alpha_s^2)$* , Phys. Rev. Lett. **93** (2004) 032002, [hep-ph/0402280].
- [25] A. Denner and S. Pozzorini, *An algorithm for the high-energy expansion of multi-loop diagrams to next-to-leading logarithmic accuracy*, Nucl. Phys. **B717** (2005) 48–85, [hep-ph/0408068].
- [26] C. Anastasiou, K. Melnikov, and F. Petriello, *Higgs boson production at hadron colliders: Differential cross sections through next-to-next-to-leading order*, Phys. Rev. Lett. **93** (2004) 262002, [hep-ph/0409088].
- [27] M. Czakon, J. Gluza, and T. Riemann, *Master integrals for massive two-loop Bhabha scattering in QED*, Phys. Rev. **D71** (2005) 073009, [hep-ph/0412164].
- [28] C. Anastasiou, K. Melnikov, and F. Petriello, *Fully differential higgs boson production and the di-photon signal through next-to-next-to-leading order*, Nucl. Phys. **B724** (2005) 197–246, [hep-ph/0501130].
- [29] C. Anastasiou, K. Melnikov, and F. Petriello, *The electron energy spectrum in muon decay through $O(\alpha^2)$* , JHEP **09** (2007) 014, [hep-ph/0505069].
- [30] G. Heinrich, *Towards $e^+e^- \rightarrow 3$ jets at NNLO by sector decomposition*, Eur. Phys. J. **C48** (2006) 25–33, [hep-ph/0601062].

- [31] K. Melnikov and F. Petriello, *The W boson production cross section at the LHC through $O(\alpha_s^2)$* , *Phys. Rev. Lett.* **96** (2006) 231803, [[hep-ph/0603182](#)].
- [32] C. Anastasiou, S. Beerli, S. Bucherer, A. Daleo, and Z. Kunszt, *Two-loop amplitudes and master integrals for the production of a Higgs boson via a massive quark and a scalar-quark loop*, *JHEP* **01** (2007) 082, [[hep-ph/0611236](#)].
- [33] M. Czakon, J. Gluza, and T. Riemann, *The planar four-point master integrals for massive two-loop Bhabha scattering*, *Nucl. Phys.* **B751** (2006) 1–17, [[hep-ph/0604101](#)].
- [34] M. Awramik, M. Czakon, and A. Freitas, *Electroweak two-loop corrections to the effective weak mixing angle*, *JHEP* **11** (2006) 048, [[hep-ph/0608099](#)].
- [35] M. Awramik, M. Czakon, and A. Freitas, *Bosonic corrections to the effective weak mixing angle at $O(\alpha^2)$* , *Phys. Lett.* **B642** (2006) 563–566, [[hep-ph/0605339](#)].
- [36] R. Boughezal and M. Czakon, *Single scale tadpoles and $O(G_F m(t)^2 \alpha_s^3)$ corrections to the rho parameter*, *Nucl. Phys.* **B755** (2006) 221–238, [[hep-ph/0606232](#)].
- [37] A. Denner, B. Jantzen, and S. Pozzorini, *Two-loop electroweak next-to-leading logarithmic corrections to massless fermionic processes*, *Nucl. Phys.* **B761** (2007) 1–62, [[hep-ph/0608326](#)].
- [38] K. Melnikov and F. Petriello, *Electroweak gauge boson production at hadron colliders through $O(\alpha_s^2)$* , *Phys. Rev.* **D74** (2006) 114017, [[hep-ph/0609070](#)].
- [39] C. Anastasiou, G. Dissertori, and F. Stockli, *NNLO QCD predictions for the $H \rightarrow WW \rightarrow ll\nu\nu$ signal at the LHC*, *JHEP* **09** (2007) 018, [[hep-ph/0707.2373](#)].
- [40] C. Anastasiou, G. Dissertori, F. Stockli, and B. R. Webber, *QCD radiation effects on the $H \rightarrow WW \rightarrow l\nu l\nu$ signal at the LHC*, *JHEP* **03** (2008) 017, [[hep-ph/0801.2682](#)].
- [41] K. Melnikov, *$O(\alpha_s^2)$ corrections to semileptonic decay $b \rightarrow cl\bar{\nu}_l$* , [[hep-ph/0803.0951](#)].
- [42] C. Anastasiou, S. Beerli, and A. Daleo, *The two-loop QCD amplitude $gg \rightarrow h, H$ in the Minimal Supersymmetric Standard Model*, [[hep-ph/0803.3065](#)].
- [43] V. A. Smirnov, *Analytical result for dimensionally regularized massless on-shell double box*, *Phys. Lett.* **B460** (1999) 397–404, [[hep-ph/9905323](#)].
- [44] J. B. Tausk, *Non-planar massless two-loop Feynman diagrams with four on-shell legs*, *Phys. Lett.* **B469** (1999) 225–234, [[hep-ph/9909506](#)].
- [45] T. Gehrmann and E. Remiddi, *Two-loop master integrals for $\gamma^* \rightarrow 3$ jets: The planar topologies*, *Nucl. Phys.* **B601** (2001) 248–286, [[hep-ph/0008287](#)].
- [46] T. Gehrmann and E. Remiddi, *Two-loop master integrals for $\gamma^* \rightarrow 3$ jets: The non-planar topologies*, *Nucl. Phys.* **B601** (2001) 287–317, [[hep-ph/0101124](#)].

- [47] L. W. Garland, T. Gehrmann, E. W. N. Glover, A. Koukoutsakis, and E. Remiddi, *The two-loop QCD matrix element for $e^+e^- \rightarrow 3$ jets*, *Nucl. Phys.* **B627** (2002) 107–188, [[hep-ph/0112081](#)].
- [48] V. A. Smirnov, *Analytical result for dimensionally regularized massless master non-planar double box with one leg off shell*, *Phys. Lett.* **B500** (2001) 330–337, [[hep-ph/0011056](#)].
- [49] V. A. Smirnov, *Analytical result for dimensionally regularized massive on-shell planar double box*, *Phys. Lett.* **B524** (2002) 129–136, [[hep-ph/0111160](#)].
- [50] A. I. Davydychev and V. A. Smirnov, *Analytical evaluation of certain on-shell two-loop three-point diagrams*, *Nucl. Instrum. Meth.* **A502** (2003) 621–623, [[hep-ph/0210171](#)].
- [51] T. Binoth and G. Heinrich, *Numerical evaluation of multi-loop integrals by sector decomposition*, *Nucl. Phys.* **B680** (2004) 375–388, [[hep-ph/0305234](#)].
- [52] G. Heinrich and V. A. Smirnov, *Analytical evaluation of dimensionally regularized massive on-shell double boxes*, *Phys. Lett.* **B598** (2004) 55–66, [[hep-ph/0406053](#)].
- [53] V. A. Smirnov, *Analytical result for dimensionally regularized massless on-shell planar triple box*, *Phys. Lett.* **B567** (2003) 193–199, [[hep-ph/0305142](#)].
- [54] T. Gehrmann, G. Heinrich, T. Huber, and C. Studerus, *Master integrals for massless three-loop form factors: One-loop and two-loop insertions*, *Phys. Lett.* **B640** (2006) 252–259, [[hep-ph/0607185](#)].
- [55] G. Heinrich, T. Huber and D. Maitre, *Phys. Lett.* **B662** (2008) 344 [[\[hep-ph\] 0711.3590](#)].
- [56] A. Ferroglia, M. Passera, G. Passarino, and S. Uccirati, *All-purpose numerical evaluation of one-loop multi-leg Feynman diagrams*, *Nucl. Phys.* **B650** (2003) 162–228, [[hep-ph/0209219](#)].
- [57] T. Binoth, G. Heinrich, and N. Kauer, *A numerical evaluation of the scalar hexagon integral in the physical region*, *Nucl. Phys.* **B654** (2003) 277–300, [[hep-ph/0210023](#)].
- [58] A. Lazopoulos, K. Melnikov, and F. J. Petriello, *NLO QCD corrections to the production of t - \bar{t} - Z in gluon fusion*, [[hep-ph\] 0709.4044](#)].
- [59] A. Lazopoulos, K. Melnikov, and F. Petriello, *QCD corrections to tri-boson production*, *Phys. Rev.* **D76** (2007) 014001, [[hep-ph/0703273](#)].
- [60] D. E. Soper, *QCD calculations by numerical integration*, *Phys. Rev. Lett.* **81** (1998) 2638–2641, [[hep-ph/9804454](#)].
- [61] D. E. Soper, *Techniques for QCD calculations by numerical integration*, *Phys. Rev.* **D62** (2000) 014009, [[hep-ph/9910292](#)].
- [62] T. Binoth, J. P. Guillet, G. Heinrich, E. Pilon, and C. Schubert, *An algebraic / numerical formalism for one-loop multi-leg amplitudes*, *JHEP* **10** (2005) 015, [[hep-ph/0504267](#)].

- [63] Z. Nagy and D. E. Soper, *Numerical integration of one-loop Feynman diagrams for N-photon amplitudes*, *Phys. Rev.* **D74** (2006) 093006, [[hep-ph/0610028](#)].
- [64] C. Anastasiou, S. Beerli, and A. Daleo, *Evaluating multi-loop Feynman diagrams with infrared and threshold singularities numerically*, *JHEP* **05** (2007) 071, [[hep-ph/0703282](#)].
- [65] H. Hironaka, *Resolution of singularities of an algebraic variety over a field of characteristic zero*, *Ann. Math.* **79**, (1964), 109.
- [66] C. Bogner and S. Weinzierl, *Periods and Feynman integrals*, [[hep-th](#)] **0711.4863**.
- [67] A. D. Kennedy, T. Binoth, and T. Rippon, *Automating renormalization of quantum field theories*, [[hep-ph](#)] **0712.1016**.
- [68] W. E. Caswell and A. D. Kennedy, *The Asymptotic Behaviour of Feynman Integrals*, *Phys. Rev.* **D28** (1983) 3073.
- [69] A. D. Kennedy, *A simple proof of the BPH theorem*, [hep-th/9612113](#).
- [70] K. Ebrahimi-Fard and D. Kreimer, *Hopf algebra approach to Feynman diagram calculations*, *J. Phys.* **A38** (2005) R385–R406, [[hep-th/0510202](#)].
- [71] G. Heinrich, *A numerical method for NNLO calculations*, *Nucl. Phys. Proc. Suppl.* **116** (2003) 368–372, [[hep-ph/0211144](#)].
- [72] N. Bogoliubov and D. Shirkov, *Introduction to the theory of quantized fields*. Wiley-Interscience, New York, 1959.
- [73] C. Itzykson and J. B. Zuber, *Quantum Field Theory*. McGraw-Hill (International Series in Pure and Applied Physics), New York, 1980.
- [74] N. Nakanishi, *Graph Theory and Feynman Integrals*. Gordon and Breach, New York, 1971.
- [75] A. I. Davydychev, *A simple formula for reducing Feynman diagrams to scalar integrals*, *Phys. Lett.* **B263** (1991) 107–111.
- [76] O. V. Tarasov, *A new approach to the momentum expansion of multiloop Feynman diagrams*, *Nucl. Phys.* **B480** (1996) 397–412, [[hep-ph/9606238](#)].
- [77] O. Zavalov, *Renormalized Quantum Field Theory*. Kluwer, 1990.
- [78] O. V. Tarasov, *Connection between Feynman integrals having different values of the space-time dimension*, *Phys. Rev.* **D54** (1996) 6479–6490, [[hep-th/9606018](#)].
- [79] L. D. Landau, *On analytic properties of vertex parts in quantum field theory*, *Nucl. Phys.* **13** (1959) 181–192.
- [80] R. J. Eden, P. V. Landshoff, D. I. Olive, and J. C. Polkinghorne, *The Analytic S-Matrix*. Cambridge University Press, 1966.
- [81] F. V. Tkachov, *Landau equations and asymptotic operation*, *Int. J. Mod. Phys.* **A14** (1999) 683–715, [[hep-ph/9703423](#)].

- [82] I. Gelfand and G. Shilov, *Generalized Functions*, vol. 1. Academic Press, New York, 1964.
- [83] E. Byckling and K. Kajantie, *Particle Kinematics*. John Wiley & Sons, 1973.
- [84] E. Byckling and K. Kajantie, *Reductions of the phase-space integral in terms of simpler processes*, *Phys. Rev.* **187** (1969) 2008–2016.
- [85] A. Erdelyi (ed.), *Higher transcendental functions*, vol. 1. McGraw-Hill, New York, 1953.
- [86] T. Huber and D. Maitre, *HypExp, a Mathematica package for expanding hypergeometric functions around integer-valued parameters*, *Comput. Phys. Commun.* **175** (2006) 122–144, [[hep-ph/0507094](#)].
- [87] G. Heinrich, *A numerical approach to infrared divergent multi-parton phase space integrals*, *Nucl. Phys. Proc. Suppl.* **135** (2004) 290–294, [[hep-ph/0406332](#)].
- [88] A. Gehrmann-De Ridder, T. Gehrmann, E. W. N. Glover, and G. Heinrich, *Second-order QCD corrections to the thrust distribution*, *Phys. Rev. Lett.* **99** (2007) 132002, [[hep-ph](#)] 0707.1285].
- [89] A. Gehrmann-De Ridder, T. Gehrmann, E. W. N. Glover, and G. Heinrich, *NNLO corrections to event shapes in e^+e^- annihilation*, *JHEP* **12** (2007) 094, [[hep-ph](#)] 0711.4711].
- [90] A. Gehrmann-De Ridder, T. Gehrmann, E. W. N. Glover, and G. Heinrich, *Infrared structure of $e^+e^- \rightarrow 3$ jets at NNLO*, *JHEP* **11** (2007) 058, [[hep-ph](#)] 0710.0346].
- [91] A. G.-D. Ridder, T. Gehrmann, E. W. N. Glover, and G. Heinrich, *Jet rates in electron-positron annihilation at $O(\alpha_s^3)$ in QCD*, *Phys. Rev. Lett.* **100** (2008) 172001, [[hep-ph](#)] 0802.0813].
- [92] A. Gehrmann-De Ridder, T. Gehrmann, and E. W. N. Glover, *Antenna subtraction at NNLO*, *JHEP* **09** (2005) 056, [[hep-ph/0505111](#)].